

On the two-proton emission of ^{45}Fe - a new type of radioactivity

J. Giovinazzo, B. Blank, M. Chartier*, S. Czajkowski, A. Fleury, M.J. Lopez Jimenez†, M.S. Pravikoff, J.-C. Thomas
CEN Bordeaux-Gradignan, Le Haut-Vigneau, F-33175 Gradignan Cedex, France

F. de Oliveira Santos, M. Lewitowicz, V. Maslov‡, M. Stanoiu
Grand Accélérateur National d'Ions Lourds, B.P. 5027, F-14076 Caen Cedex, France

R. Grzywacz§, M. Pfützner
Institute of Experimental Physics, University of Warsaw, PL-00-681 Warsaw, Poland

C. Borcea
IAP, Bucharest-Magurele, P.O. Box MG6, Rumania

B.A. Brown
Department of Physics and Astronomy and National Superconducting Cyclotron Laboratory, Michigan State University, East Lansing, Michigan 48824-1321, USA

In an experiment at the SISSI-LISE3 facility of GANIL, the decay of the proton drip-line nucleus ^{45}Fe has been studied after projectile fragmentation of a ^{58}Ni primary beam at 75 MeV/nucleon impinging on a natural nickel target. Fragment-implantation events have been correlated with radioactive decay events in a 16×16 pixel silicon strip detector on an event-by-event basis. The decay-energy spectrum of ^{45}Fe implants shows a distinct peak at (1.06 ± 0.04) MeV with a half-life of $T_{1/2} = (4.7_{-1.4}^{+3.4})$ ms. None of the events in this peak is in coincidence with β particles which were searched for in a detector next to the implantation detector. For a longer correlation interval, daughter decays of the two-proton daughter ^{43}Cr can be observed after ^{45}Fe implantation. The decay energy for ^{45}Fe agrees nicely with several theoretical predictions for two-proton emission. Barrier-penetration calculations slightly favour a di-proton emission picture over an emission of two individual protons and point thus to a ^2He emission mode.

PACS numbers: 23.50.+z, 23.90.+w, 21.10.-k, 27.40.+z

An ensemble of protons and neutrons can form a nucleus stable against any radioactive decay only if a subtle equilibrium between the number of protons and neutrons is respected. If this equilibrium condition is not respected in a nucleus, it becomes radioactive. For small deviations from equilibrium, the nuclei decay by β decay. The limits of stability, the drip lines, are reached if the nuclear forces are no longer able to bind an ensemble of nucleons with a too large neutron or proton excess. Whereas for

heavy nuclei, e.g. α decay, ^{14}C radioactivity or fission occurs, unstable proton-rich nuclei may decay by emission of one proton for odd-Z nuclei or of two protons for even-Z nuclei from their ground states. The one-proton ground-state decay has been observed for the first time at GSI Darmstadt in 1981 [1,2]. Meanwhile almost 30 cases of proton radioactivity have been identified for odd-Z nuclei beyond the proton drip line between $Z=51$ and $Z=83$ [3] allowing e.g. to establish the sequence of shell-model single-particle levels beyond the proton drip line.

Two-proton (2p) radioactivity is predicted since 1960 [4] to occur for even-Z proton-rich nuclei beyond the drip line. Due to the pairing energy, the 2p candidates cannot decay by a sequential emission of two protons as the one-proton daughter is energetically not accessible. Therefore, only a simultaneous two-proton emission is possible which can take place in two different ways: i) by an isotropic emission of the two protons which then have no angular correlation, i.e. they fill the whole phase space available, but in order to easily penetrate through the Coulomb and centrifugal barrier of the daughter nucleus they share most probably equally the decay energy; ii) by a correlated emission where in the decay the ^2He resonance is formed which decays either already under the Coulomb and centrifugal barrier or outside the barrier. In both cases, a zero energy difference between the two protons is most likely. However, for a ^2He emission, a small relative angle between the two protons might be observable.

Recent theoretical work [5–7] showed that ^{45}Fe , ^{48}Ni , and ^{54}Zn are the best candidates for two-proton ground-state decay as their 2p Q values are about 1.1-1.8 MeV, whereas one-proton emission is either energetically forbidden or extremely disfavoured due to small one-proton decay energies and very narrow intermediate states.

For light nuclei, the Coulomb and centrifugal barriers for proton emission are smaller and the width of the ground states of these nuclei become large. Thus, one-

*present address: Oliver Lodge Laboratory, Department of Physics, University of Liverpool, Liverpool, L69 7ZE, UK

†present address: CEA/DPTA/SPN Bruyres-le-Chitel, F-91680 Bruyres-le-Chitel, France

‡present address: Flerov Laboratory of Nuclear Reactions, Joint Institute for Nuclear Research, 141980 Dubna, Russia

§present address: Physics Division, ORNL, Oak Ridge, TN 37831-6371, USA

proton emission is energetically possible through the tails of broad intermediate states even for even- Z nuclei. This has been observed experimentally for ${}^6\text{Be}$ [8] and ${}^{12}\text{O}$ [9]. In both cases, the emission pattern is compatible with a simultaneous uncorrelated decay into the available phase space. Two-proton emission from excited states has been observed in eight cases after β decay (see [10] for a recent reference) as well as after inelastic excitation of ${}^{14}\text{O}$ [11] and of ${}^{18}\text{Ne}$ [12]. In all cases, the experimental data are either not precise enough to indicate a detailed decay pattern or compatible with a sequential or three-body picture with half-lives as short as 10^{-21}s .

With the advent of projectile-fragmentation facilities equipped with powerful separators for in-flight isotope separation, medium-mass proton drip-line nuclei came into experimental reach and two of the above mentioned most promising candidates, ${}^{45}\text{Fe}$ [13] and ${}^{48}\text{Ni}$ [14], could be observed. In addition, part of the decay strength of ${}^{45}\text{Fe}$ was observed [15] in the experiment designed to identify for the first time ${}^{48}\text{Ni}$ [14]. However, due to the set-up of the electronics in this experiment, two-proton events triggered the data acquisition only with a very low probability (five possible events at about 1.1 MeV [15]).

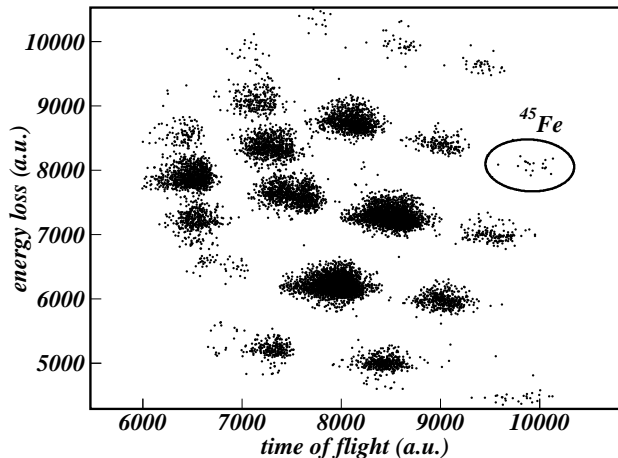


FIG. 1. Two-dimensional fragment identification spectrum for the present experiment. The implantation events are plotted as a function of their time-of-flight between one channel-plate detector and the silicon stack and their energy loss in the first silicon detector. The figure shows only part of the data.

In an experiment performed in June/July 2000 at the SISSI-LISE3 facility of GANIL, we used the projectile fragmentation of a ${}^{58}\text{Ni}$ primary beam at 75 MeV/nucleon to produce proton-rich nuclei in the range $Z=20-28$. After production in a ${}^{nat}\text{Ni}$ target (240 μm in thickness) located in the SISSI device, the fragments of interest were selected by the Alpha/LISE3 separator equipped with an intermediate beryllium degrader (50 μm). At the focus of the LISE3 separator, a set-up was mounted to identify (see figure 1) and stop the fragments as well as to study their radioactive decays.

This set-up consisted in two channel-plate detection systems for timing purposes mounted at a first LISE focal point 22.9 m upstream from the final focus, a sequence of four silicon detectors (E1: 300 μm , E2: 300 μm , E3: 300 μm , E4: 6mm, respectively) with the third one being a silicon-strip detector with 16×16 x-y strips with a pitch of 3 mm, and a Germanium array in close geometry. The silicon detectors were equipped with two parallel electronic chains with different gains, one for heavy-fragment identification and the other for decay spectroscopy.

The fragments of interest were stopped in the third silicon detector of the telescope and identified on an event-by-event basis by means of their flight times and of their energy loss in all detectors of the telescope (see [14,15]). Implantation events were triggered by detectors E1 and E2, whereas radioactive decay events were triggered either by the detector E3 or by the adjacent silicon detector E4. The efficiency to observe a β particle in the E4 detector for a β decay occurring in the implantation detector is about 30%. The γ energy calibration and detection efficiency was obtained with standard calibration sources. The efficiency was about 1.6% at 1.3 MeV.

In a 36 h run, 22 ${}^{45}\text{Fe}$ implantations were identified. Due to a rather low implantation rate of much less than one radioactive isotope per second in each pixel, an implantation-decay correlation could be performed on an event-by-event basis with each decay event being correlated to each implantation in the same x-y pixel having occurred less than a well-defined maximum time interval before the decay event.

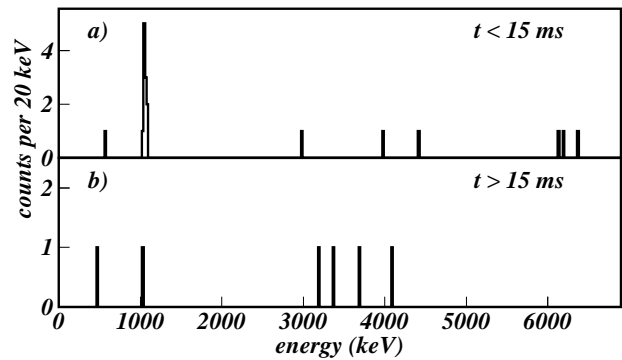


FIG. 2. Decay-energy spectrum correlated with ${}^{45}\text{Fe}$ implantation. Spectrum a) is obtained under the condition that the radioactive decay occurs faster than 15 ms after implantation, whereas spectrum b) contains decay events with decay times between 15 ms and 100 ms. The peak at 1.06 MeV is clearly identified as being due to a fast decay.

Figure 2a shows the decay-energy spectrum correlated with implants of ${}^{45}\text{Fe}$ where only decay events occurring less than 15 ms after a ${}^{45}\text{Fe}$ implantation were analysed. The spectrum exhibits a pronounced peak at (1.06 ± 0.04) MeV with only a very few other counts. In contrary, in the spectrum in figure 2b conditioned by a decay time in the interval between 15 ms and 100 ms,

the 1.06 MeV peak has almost completely disappeared and other events higher in decay energy show up. These counts are consistent with the decay-energy spectrum of ^{43}Cr [15], the 2p daughter of ^{45}Fe . The 1.06 MeV peak, however, seems to originate only from the fast decay of ^{45}Fe . In addition, the events in this peak have no coincident β -particle signals in the adjacent detector E4 (see figure 3a) beyond the noise level, whereas these coincident β particles can be observed for the β decay of ^{46}Fe implants analysed with a similar condition in energy for the E3 detector. For 12 ^{46}Fe events in the decay-energy interval 0.875 - 1.3 MeV, six coincident β particles can be identified in the E4 detector (see figure 3b). As the β -decay end-point energies are roughly the same for ^{45}Fe and ^{46}Fe and therefore similar β -detection efficiencies can be assumed, the non-observation of β particles in coincidence with the 1.06 MeV peak alone is a strong indication that this peak originates from a direct two-proton ground-state decay of ^{45}Fe . The probability to miss all β particles for the 12 events in the peak is as low as 1.4%. Although the γ -detection efficiency was rather low, it is worth mentioning that none of the 12 events in the 1.06 MeV peak is in coincidence with a γ ray.

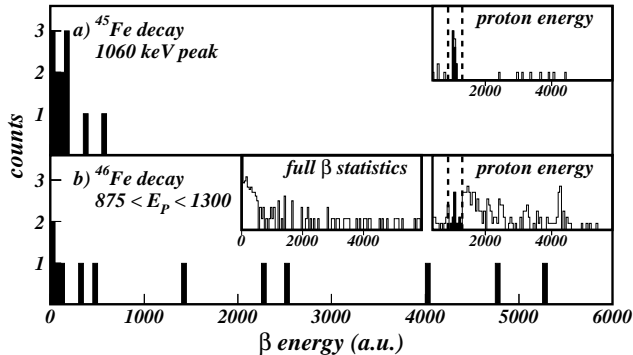


FIG. 3. a) β -particle spectrum from the 6mm-thick detector E4 in coincidence with events in the peak at 1.06 MeV. b) Similar spectrum obtained after ^{46}Fe implantation conditioned by a decay-energy range in the E3 detector of $E = 0.875 - 1.3$ MeV, which yields the same statistics as for the 1.06 MeV peak of ^{45}Fe . The insets show the decay-energy spectrum for the two nuclei with the dark area and the dotted lines indicating the decay-energy condition applied to generate the β spectra as well as the full-statistics ^{46}Fe β spectrum.

The observation of only twelve events in the peak at 1.06 MeV indicates that the branching ratio for 2p decay of ^{45}Fe is not hundred percent, in agreement with theoretical prediction of a β -decay half-life of about 7 ms [6]. However, dead-time losses (the data-acquisition dead time is about 0.5 ms) make us lose about 3-4 events. The dead zone between two strips of the implantation detector is another possible source of losses. The events with an energy above 6 MeV (see figure 2a) decay with a half-life compatible with the one of ^{45}Fe and are therefore must likely β -delayed events. With this information, a branching ratio for 2p emission of 70-80% can be esti-

ated.

The observation of a pronounced peak at 1.06 MeV from the decay of ^{45}Fe is a strong additional indication that ^{45}Fe is not decaying by a β -delayed mode alone as does ^{46}Fe [15] with a more complex decay-energy spectrum. In addition, the width of the ^{45}Fe peak (60 ± 10 keV) is about 40% smaller than β -delayed one-proton peaks from neighboring nuclei. Although the statistics is limited, this indicates that the ^{45}Fe peak is not broadened due to β pile-up.

The decay-time spectrum of ^{45}Fe gated by the 1.06 MeV peak is shown in figure 4. A one-component fit with an exponential yields a half-life for ^{45}Fe of $T_{1/2} = (4.7^{+3.4}_{-1.4})$ ms. The decay-time spectrum of events up to 100 ms after a ^{45}Fe implantation can be fitted by taking into account the decay of ^{45}Fe and its 2p daughter ^{43}Cr . The half-life then is $(5.7^{+2.7}_{-1.4})$ ms.

The energy of the peak at 1.06 MeV agrees nicely with Q_{2p} value predictions from Brown [5] of 1.15(9) MeV, from Ormand [6] of 1.28(18) MeV, and from Cole [7] of 1.22(5) MeV. These models use the isobaric-multiplet mass equation and shell-model calculations to determine masses of proton-rich nuclei from their neutron-rich mirror partners. Q-value predictions from models aiming at predicting masses for the entire chart of nuclei are in less good agreement with our present result. All the 2p Q-value predictions are summarized in figure 5, where they are used in barrier-penetration calculations using the simple di-proton model for two-proton emission (the model used in [5] with $R = 4.2$ fm).

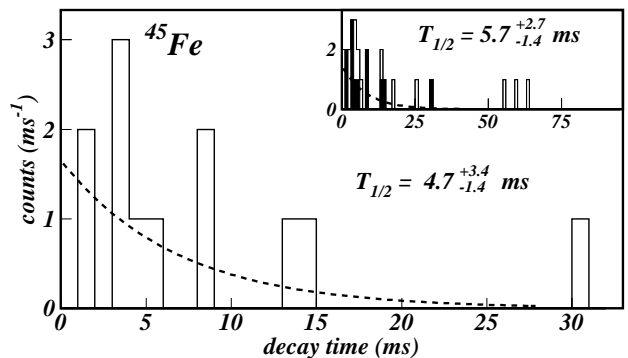


FIG. 4. Decay-time spectrum of ^{45}Fe . The twelve events in the 1.06 MeV peak are fitted by a one-component exponential using the maximum likelihood procedure. The half-life thus obtained is $(4.7^{+3.4}_{-1.4})$ ms. A fit, including the daughter decay, of all correlated event up to 100 ms after ^{45}Fe implantation (see inset) yields a half-life of $(5.7^{+2.7}_{-1.4})$ ms for ^{45}Fe and a value consistent with literature [15] for ^{43}Cr . The dark shaded counts originate from the 1.06 MeV peak.

For $E_p = 1.06 \pm 0.04$ MeV, these calculations predict a di-proton barrier penetration half-life of $(0.2^{+0.3}_{-0.1})$ ms, if one assumes a spectroscopic factor of unity. Brown [5,16] calculated a spectroscopic factor of 0.195 for a direct 2p decay of ^{45}Fe which increases the barrier tunnel time to

a predicted half-life of $(1.2_{-0.5}^{+1.5})$ ms.

We have also used the R-matrix formulation of Barker [23] both in its simple form, equivalent to the di-proton decay model discussed above, and in a more realistic form which includes the s-wave resonance of the two protons. In the R-matrix we need to choose a channel radius a and an associated dimensionless reduced width θ_{sp}^2 (Eq. 16 of [24]). For consistency we take $a = 4.2$ fm which is a region of the resonance wave function where $\theta_{sp}^2 \approx 1$. With $S = 0.195$ we obtain a half-life of $(1.7_{-0.5}^{+2.3})$ ms in the simple model, and (8_{-6}^{+22}) s in the s-wave resonance model. The reduction in the phase space due to the two-proton resonance increases the lifetime by a factor of 4000. Grigorenko et al. [25] studied the emission of two protons from ^{48}Ni in a three-body model. They find that the half-life for the same Q_{2p} value increases by about three orders of magnitude when going from a simple di-proton model to the more advanced three-body model. Thus the models which include the interaction between two-protons appear to give a lifetime which is much longer than the observed value.

A sequential decay seems to be excluded for ^{45}Fe , as the intermediate state, the ground state of ^{44}Mn , is, depending on the prediction used, either not in the allowed region or at the very limit of the allowed region. The model predictions [5–7] range from $Q_{1p} = -24$ keV to $+10$ keV. As the intermediate state is most probably rather narrow (barrier-penetration calculations yield a value of about $\Gamma = 50$ meV), the first proton would have a very long half-life (hours or even days), which makes this decay mode very unlikely.

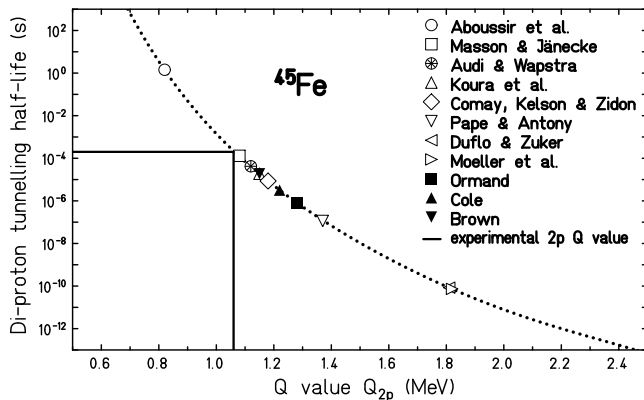


FIG. 5. Barrier-penetration half-life as a function of the two-proton Q value, Q_{2p} , for ^{45}Fe . The barrier penetration was calculated by assuming a spectroscopic factor of unity. Different model predictions [5–7, 17–22] were used for Q_{2p} . The experimentally observed Q value of ^{45}Fe implies a di-proton barrier-penetration half-life of 0.2 ms.

In conclusion, we have studied the decay of ^{45}Fe in an experiment where we measured its decay energy yielding a peak at 1.06 MeV, a half-life of 4.7 ms, and, in particular, no coincident β particle or γ ray for the events in the decay-energy peak. In addition, strong indications for the decay of the 2p daughter, ^{43}Cr , after implantation

of ^{45}Fe are found. Additional support comes from the width of the ^{45}Fe peak. The energy of the observed peak is in reasonable agreement with theoretical predictions for the 2p decay energy. A consistent picture arises, if one assumes that a two-proton ground-state emission occurs. Simple model calculations favor the observed decay mode to be a ^2He /di-proton emission.

Whereas the two-proton ground-state decay of ^{45}Fe seems to be established with the present data, future high-statistics data should definitively allow to conclude on the nature of the two-proton decay, ^2He emission or three-body decay. This question can be addressed in an experiment, which measures the individual proton energies and the relative-angle distribution for the two protons emitted which should be either isotropic (three-body decay) or forward-peaked (^2He emission).

It should be mentioned that similar results, although with less statistics and a lower energy resolution, were also obtained at the FRS of GSI [26].

We would like to acknowledge the continuous effort of the whole GANIL staff for ensuring a smooth running of the experiment. This work was supported in part by the Polish Committee of Scientific Research under grant KBN 2 P03B 036 15, the contract between IN2P3 and Poland, the NSF grant PHY-00-7911, as well as by the Conseil Régional d'Aquitaine.

-
- [1] S. Hofmann *et al.*, Z. Phys. **A305**, 111 (1982).
 - [2] O. Klepper *et al.*, Z. Phys. **A305**, 125 (1982).
 - [3] P. Woods and C. Davids, Annu. Rev. Nucl. Part. Sci. **47**, 541 (1997).
 - [4] V.I. Goldansky, Nucl. Phys. **19**, 482 (1960).
 - [5] B.A. Brown, Phys. Rev. C **43**, R1513 (1991).
 - [6] W.E. Ormand, Phys. Rev. C **53**, 214 (1996).
 - [7] B.J. Cole, Phys. Rev. C **54**, 1240 (1996).
 - [8] O.V. Bochkarev *et al.*, Sov. J. Nucl. Phys. **55**, 955 (1992).
 - [9] A. Azhari, R. Kryger, and M. Thoennessen, Phys. Rev. C **58**, 2568 (1998).
 - [10] H. Fynbo *et al.*, Nucl. Phys. A **677**, 38 (2000).
 - [11] C. Bain *et al.*, Phys. Lett. **373B**, 35 (1996).
 - [12] J. Gomez del Campo *et al.*, Phys. Rev. Lett. **86**, 43 (2001).
 - [13] B. Blank *et al.*, Phys. Rev. Lett. **77**, 2893 (1996).
 - [14] B. Blank *et al.*, Phys. Rev. Lett. **84**, 1116 (2000).
 - [15] J. Giovinazzo *et al.*, Eur. Phys. J. A **10**, 73 (2001).
 - [16] B.A. Brown, Phys. Rev. C **44**, 924 (1991).
 - [17] P. Haustein, At. Data Nucl. Data Tab. **39**, 185 (1988).
 - [18] P. Möller, J. R. Nix, W. D. Myers, and W. J. Swiatecki, At. Data Nucl. Data Tab. **59**, 185 (1995).
 - [19] J. Duflo and A. Zuker, Phys. Rev. C **52**, R23 (1995).
 - [20] Y. Aboussir, J. Pearson, A. Dutta, and F. Tondeur, At. Data Nucl. Data Tab. **61**, 127 (1995).
 - [21] G. Audi and A. H. Wapstra, Nucl. Phys. **A625**, 1 (1997).
 - [22] H. Koura, M. Uno, T. Tachibana, and M. Yamada, Nucl. Phys. **A674**, 47 (2000).
 - [23] F.C. Barker, Phys. Rev. C **63**, 047303 (2001).
 - [24] F.C. Barker, Phys. Rev. C **59**, 535 (1999).
 - [25] L. Grigorenko *et al.*, Phys. Rev. Lett. **85**, 22 (2000).
 - [26] M. Pfützner *et al.*, to be published.